УДК 678.7

A. A. Olkhov, B. M. Rumyantsev, G. E. Zaikov,
A. A. Ischenko, V. F. Shkodich, A. M. Kochnev

STRUCTURE AND PHOTOELECTRIC PROPERTIES OF POLYIMIDES BASED ON N,N',N",N"'- SUBSTITUTED PAREPHENYLENEDIAMINE AND DIANHYDRIDES OF AROMATIC TETRACARBOXYLIC ACIDS

Key words: electrophotographic method, polyimides, Suzuki coupling reaction, photoelectric characteristics, photoelectric sensitivity, charge transfer complex, photogeneration quantum yield, photogeneration mechanism, cation-radical, anion-radical, photovoltaic characteristics.

The photoelectric characteristics of the newly synthesized polyimides PI are investigated by using the electrophotographic method. A novel conjugated polymers, polyimides based on N,N',N",N"'-substituted paraphenylenediamine and dianhydrides of aromatic tetracarboxylic acids, was prepared via Suzuki coupling reaction. The polymer exhibits excellent solubility in common organic solvent, and has high thermal stability such as T_{d10} at 453 ^{0}C in nitrogen atmosphere and T_g at about 140 ^{0}C. The photoelectric sensitivity of the PI films (3 □m thickness) is observed in the UV, and visible spectral regions, due to the interactions with charge transfer between donor and acceptor fragments of the PI chains (formation of charge transfer complex, CTC). Study of the photogeneration quantum yield field dependence gives the evidence that the photogeneration mechanism is a field assisted thermo-dissociation of radical ion pairs kinetically associated with the excited CTC. The second important mechanism of photogeneration is photostimulation of long-lived stable cation-radicals of the donor PI fragments, representing the hole (major carriers) captured by deep centers (photostimulated currents). Accumulation of the cation-radicals in the dark and photoprocesses leads to the dependence of photovoltaic characteristics on the number of charge-discharge cycles of the sample.

Ключевые слова: электрофотографический метод, полиимиды, реакция сочетания Сузуки, фотоэлектрические характеристики, фотоэлектрическая чувствительность, комплексный перенос заряда, фотогенерация квантовый выход, механизм фотогенерации, катион-радикальные, анион-радикальные, фотоэлектрические характеристики.

Фотоэлектрические характеристики синтезированных полиимидов (ПИ) исследованы электрофотографическим методом. Новые конъюгированные полимеры, полиамиды на основе N, N', N", N" - замещенных парафенилендиамин и диангидридов тетракарбоновых ароматических кислот, были подготовлены с помощью реакции сочетания Сузуки. Полимер обладает отличной растворимостью в органическом растворителе, и имеет высокую термическую стабильность, например T_{D10} при 453 ºС в атмосфере азота и при Tg около 140ºС. Фотоэлектрическая чувствительность ПИ пленок (3μм толщина) наблюдается в УФ и видимой областях спектра, благодаря взаимодействию переноса заряда между донорными и акцепторными участками ПИ цепей (образование комплексного переноса заряда, КПЗ). Исследование области зависимости фотогенерации квантового выхода доказывает то, что механизм фотогенерации является областью, способствующей к термодиссоциации ион-радикальных пар, кинетически связанных с возбужденным КПЗ. Вторым важным механизмом фотогенерации является фотостимуляция долгоживущих стабильных катион-радикалов - участков ПИ-доноров, представляющих отверстие (основные носители), захваченное глубокими центрами (фотостимулированные токи). Накопление катион-радикалов, в темноте и фотопроцессах приводит к зависимости фотоэлектрических характеристик от количества циклов заряд-разряда образца.

Introduction

In the last two decades, p-conjugated polymers have attracted considerable interests because of their potential applications in electrochromics, [1–4] light emitting diodes, [5–9] organic thin film transistors, [10–14] photovoltaic's, [15–18] and polymer memories [19–20]. Fluorene and its analogous derivatives have drawn much attention of optoelectronics because they generally have good solubility, high luminescent efficiency, and very good charge-transfer mobility in both neutral and doped states [21–24]. However, it is also known that they have drawbacks such as unsatisfied thermal stability and excimers formation in the solid state [25, 26]. The applications for electrochromic conjugated polymers are quite diverse due to several favorable properties of these materials, like stable oxidation state, fast switching times, and excellent switching reproducibility [27]. These excellent properties led to the development of many technological applications such as self-darkening rear-view mirrors, adjustably darkening windows, large-scale electrochromic screens, and chameleon materials [28–30]. Electron-rich triarylamines are known to be easily oxidized to form stable polarons, and the oxidation process is always associated with a noticeable change of the coloration. Furthermore, triarylamine-based polymers are not only widely used as the hole-transport layer in electroluminescent diodes but also show interesting electrochromic behavior [31–33]. A conjugated polymer derived from the Suzuki coupling reaction with a □luorine derivative was prepared, and its general properties such as thermal and optical properties as well as electrochemical and electrochromic property were investigated and discussed earlier [34]. The high photoelectric characteristics of polyimides (PI) based on triphenylamine and its derivatives [35], and also their composites with the organic and inorganic semiconductors [36,37] (photoelectric sensitivity (PES) S, the quantum yield of the charge carrier photogeneration β, their drift length l_D, collection coefficient C(Z)) are the basis of their applications in a whole series of optoelectronic devices: photovoltaic and electroluminescent cells [38,39], photodetectors [40],

organic phototransistors [41,42]. In the present work, the photoelectric characteristics of the newly synthesized PI [34, 43] are investigated by using the electrophotographic (EPG) method [42].

Experimental

Synthesis of homopolyimides. The polyimides were prepared in the procedures similar to one described in Appendix 1. One of the examples is described as follows. To the stirred solution of 0.6g (0.883 mmol) of diamine **(4, Appendix 1)** in 5 mL of DMAc, 0.382g (0.883 mmol) of 6FDA was gradually added. The mixture was stirred at room temperature for 4 h under nitrogen atmosphere to form poly(amic acid). Chemical cyclodehydration was carried out by adding equal molar mixture of acetic anhydride and pyridine into the above-mentioned poly(amic acid) solution with stirring at room temperature for 1 h, and then treated at 100 ^{o}C for 4 h. The polymer solution was poured into methanol. The precipitate was collected by filtration, washed thoroughly with methanol, and then dried at 100 ^{o}C under vacuum.

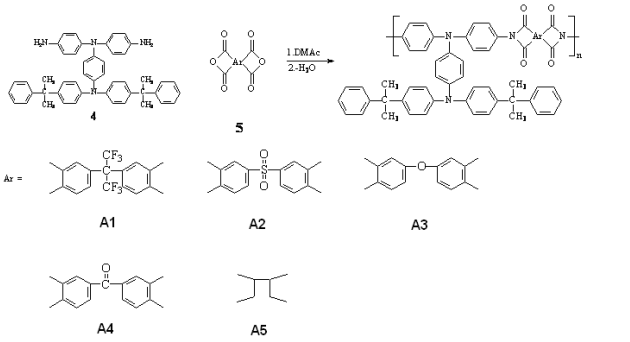

Electrophotographic study. Electrophotographic method involves the studying of the kinetics of the surface potential dark and photoinduced decay in polymer films, charged in the field of positive or negative corona discharge. The maximum potential of the charging V and the rate of the potential dark decay $(dV/dt)_D$ are determined by the dark conductivity of the films: the higher it is, the lower the V value and higher $(dV/dt)_D$ are. Potential photoinduced decay (1/I)(dV/dt) (where the I – intensity of excitation) is determined by the rate of the capacitor photodischarging formed by the ionic contact (aeroions on the film surface) as one electrode and glass conducting support (Indium Tin Oxide, ITO) as the second electrode with the induced charge of opposite sign on it. The potential photodischarging rate depends on the effective charge carrier photogeneration quantum yield in the film volume (xerographic output, β_{eff}), carrier collection efficiency on the electrodes C(Z) and the portion of the absorbed exciting light, P:

$$(1/I)\,[dV/dt - (dV/dt)_D)] = (ed/\varepsilon\varepsilon_0)\,\beta_{eff}\,P, \quad (1)$$

where $\beta_{eff} = \beta C(Z)$; C(Z) – charge carrier collection efficiency, $Z = \mu V\tau/d^2$ – ratio of the carrier drift length ($l_D = \mu V\tau/d$) to the film thickness d, μ – carrier drift mobility, τ – their lifetime, e – electron charge. The function C(Z) for the strong and weak absorption is given in [42], from which it follows that for $Z < 1$, $C(Z) = Z$, and for $Z > 1$, $C(Z) = 1$ (strong absorption) and $C(Z) = 1/2$ for weak absorption. It is observed [39], that for the polymers, β and C(Z) values usually are strongly depend on the field strength $E = V/d$. The accuracy of the β measurement was determined by the accuracy of the I, P and film thickness d measurements and was estimated ~20%. The photoelectric sensitivity (PES) S ([m^2/J]) is defined as the reciprocal value of the half decay exposure time $t_{1/2}$ of the initial charging potential V:

$$S = (It_{1/2})^{-1} = (\beta_{eff}\,Pde)/[E(h\nu)V\varepsilon\varepsilon_0], \quad (2)$$

where E(hν) – excitation photon energy. The accuracy of the S value measurement was estimated ~10% and it was determined by the accuracy of excitation intensity I measurements. Thus, the electrophotographic method makes it possible to obtain the following photoelectric characteristics of polymer samples: photoelectric sensitivity, the carrier photogeneration quantum yield (1), and from the field dependence of $\beta_{eff}(E)$ it is possible to estimate carrier drift length: at the field strength E_0, for which the change of C(Z) dependence from C(Z) = Z to C(Z) = const is observed, drift length is equal to the film thickness, $l_D = \mu E_{0\tau} = d$. Experimental setup makes it possible to determine both the optical density of the sample D_λ under monochromatic or integral excitation, and to measure also the influence of the ionic contact field on it. Knowing optical density, it is possible to estimate the portion of the absorbed excitation light energy:

$$P = 1 - \exp[-(D-D_0)], \quad (3)$$

where D is the film optical density and D_0 – equivalent optical density, caused by the light reflection from the front and rear sample surfaces as well as by light scattering. The sign of major carriers can be determined via the comparison of PES values for the positive (S^+) and negative (S^-) corona charging of free surface under the heterogeneous excitation by the strongly absorbed UV light: with $S^+ > S^-$ major carriers are holes, with $S^- > S^+$ - electrons. The PI films of 3 μm thickness were prepared by the cast of polymer solution in the chlorine – containing solvents onto the conducting ITO glass supports and the subsequent drying under the ambient conditions at 50-100 ^{0}C. The Pis under study possess good solubility and excellent film-forming properties

Results and Discussions Study of the Photoelectric Sensitivity of the PI films and its connection with the Charge Transfer Complex formation

Photoelectric sensitivity of the PI films is observed and the charge carrier photogeneration quantum yield is determined for the films of the new class of PI based on N,N',N",N"' - substituted paraphenylenediamine (electron-donor fragment D) and dianhydrides of aromatic tetracarboxylic acids (electron-acceptor fragment A). PI series denoted as PI A1 to PI A5, see list of samples above. A study of PES spectral dependence S(λ) shows that the highest sensitivity (up to 30 m^2/J) is observed at the UV region (200 – 400 nm). In the visible region (400 -700 nm) there is a PES band which collapses to the long-wave edge (Figure1).

Comparison of the PES spectral dependence with the absorption spectrum of the films evidences that PES in the visible region is due to the formation of weak electronic Donor-Acceptor (D-A) Charge-Transfer Complexes (CTC) with absorption maxima in the region of 400 – 600 nm [44]. The maxima and band absorption edge of the CTC are determined. The most

clearly expressed CTC bands are observed for PI A2 and PI A3 films with flat absorption maxima in the 500- 560 nm region. For PI A1, PI A4 and PI A5 films CTC bands are essentially weaker with flat maxima shifted to short wavelengths, 420 – 480 nm. The energy position of the long-wavelength absorption band edge of the CTC and PES is determined, which is an analogue of the band gap for semiconductors, E_g, that allows to estimate the relative affinity energy values for the acceptor fragments E_A (at the same values of the ionization potential of the donor fragments, $I_D = 7.0 - P_h = 5.5$ eV, P_h – polarization energy of holes) from the expression:

$$E_g = I_D - E_A - (P_h + P_e), \quad (4)$$

where P_e –polarization energy for electrons.

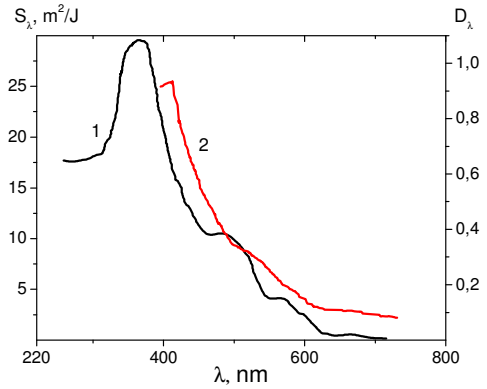

Fig. 1 - Spectra of the photoelectric sensitivity S_λ(1): (+ charging, V = 30-36 V; the number of cycles N > 10) and the optical density D_λ(2) for the film PI A2 (thickness d = 3 μm)

Table 1 - E_g and ($E_A + P_e$) values (in eV) for PI A1 – PI A5 film samples; P_e = 1.5 eV

PI A1	E_g = 2.2*	(E_A+P_e) = 3.3*
PI A2	1.9	3.6
PI A3	2.0	3.5
PI A4	2.6	2.9
PI A5	2.4	3.1

* Estimated average uncertainty for E_g and (E_A+P_e) values is 0.1 eV.

As can be seen from Table 1, the highest E_A values are observed for PI A2 and PI A3 acceptor fragments (3.6 and 3.5 eV, respectively) which characterized by the lowest E_g (1.9 and 2.0 eV) and the most pronounced CTC band as well as high PES in the visible region (up to 5 – 20 m^2/J). The PI A1, PI A4 and PI A5 films possess the lower E_A values, weaker CTC bands and lower PES (of about 1- 4 m^2/J).

These distinct spectral peaks (in the region of 440-480 nm, 540-560 nm and 640-660 nm) are registered for PI A1, PI A3, PI A5 (absorption spectrum) and PI A2 (PES spectrum, Figure1). They are ascribed in this work to the formation and accumulation of the stabilized cation-radicals (D^+) (and perhaps anion-radicals (A^-)) of polymer fragments arising in the PI as a result of the dark- and photo-processes [45]. Some evidence of this assumption is the PES found in the red region (λ > 600 nm, outside the CTC band) with a weak maximum in the absorption band of triphenylamine type cation-radical (640-660 nm) due to its photo-stimulation [45].

The photo-generation quantum yield for the UV (PI A1-PI A5) and visible spectrum (PI A1) is determined. On varying charging potential V a non-linear field dependence of photo-generation quantum yield $\beta(E) \sim E^n$ (Figure 2) is revealed. The exponent n increases with increasing excitation wavelength λ from n ~ 1.2 to n ~ 1.8 on changing λ from 257 to 547 nm, indicating that the photo-generation occurs via the field assisted thermo-dissociation (FATD) of ion pairs (IP), kinetically coupled with the excited states of the CTC:

$$\mathbf{CTC + h\upsilon_{CT} \rightarrow CTC^* \leftrightarrow [D^+ \ldots A^-] \rightarrow carriers\ (holes)} \quad (5)$$

FATD

E, T

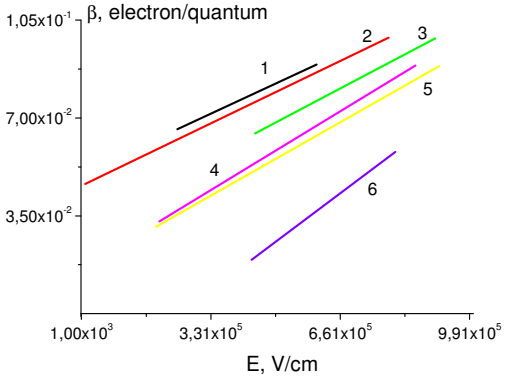

Fig. 2 - Field dependence of charge carrier photogeneration quantum yield β(E) for the PI A2 (1), PI A1 (2, 4-6) and PI A3 (3) films, under excitation by monochromatic light: 257 nm (2) and 365 nm (1, 3, and 4); 436 nm (5) and 547 nm (6). Positive charging (N > 10), the field changed by the time variation of corona. β in electrons/quanta, E in V/cm

The highest β values in the UV region (up to 0.1 in a field $E = 5.7 \cdot 10^5$ V/cm) are obtained for films PI A3 and PI A2 (β = 0.02, $E = 10^5$ V / cm). Using the geminate recombination Onsager model [46, 47] to interpret the field dependence of β(E), it is possible to determine ion-pair parameters: the initial yield Φ_0 and initial separation r_0. For films PI A1 with increasing excitation wavelength (from 257 to 547 nm) value of r_0 is reduced from 3.6 – 4.5 nm to 2.0 nm, and the value of Φ_0 increases from 0.2 to 0.7. However under excitation in the red spectral region (640-680 nm, outside of the CTC band), the value r_0 increases to 3.0 nm, which suggests that under photostimulation of stabilized cation-radical IP_1 is formed that differs the IP in the scheme (3). Comparison of the field dependences of S and β allows to conclude that for the PI films drift length of the generated carriers (holes) $l_D > d$ (3 μm) for $E > 10^5$ V/cm and hence to estimate $\mu\tau > 3 \cdot 10^{-9}$ cm^2/V. Major carriers in the studied PI – holes since under free surface excitation by strongly absorbed UV light, $S^+ > S^-$.

2. Effect of stable cation-radicals accumulation during repeating charge- discharge cycles on the photoelectric characteristics of the PI films; the observation of the photo-stimulated current (PSC). A strong dependence of the photoelectric characteristics of the samples (the

potential of charging, PES in the red region, S_{red}) on the number of charge-discharge cycles N is found: when changing N from 1 to 10, V and S_{red} values significantly (of about several times) increase (Figure 3). In the UV region the rise only V is observed; the growth of PES is very small or completely absent.

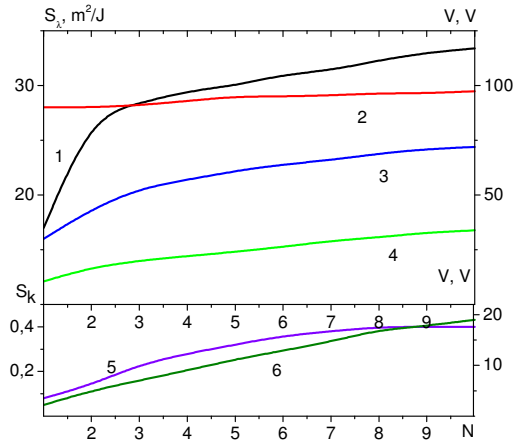

Fig. 3 - Photoelectric sensitivity in the UV (λ = 365 nm) $S_λ$ (1, 2) and red region (λ > 600 nm) S_{red} (5), as well as the maximal charge potential V (3, 4, 6) versus number of charge-discharge cycles N for films PI A5 (2, 3) and PI A2 (1, 4-6); + charging

Usually the absence of surface charging associated with the dark injection of carriers from the electrodes into the bulk of the film (holes in case of positively charged free surface), leading to a sharp increase in dark conductivity. The increase in the value of V at the positive charge indicates blocking of the dark hole injection from the free surface when N > 3 – 4. The most probable reason is the appearance in the film bulk near the electrode positively charged layer of stabilized cation-radicals (electrode polarization). The latter are holes (h^+) trapped by deep centers:

$$\text{+ Electrode+D} \xrightarrow{\text{dark injection}} \text{h}^+\text{ (mobile hole)} \xrightarrow{\text{capture}} \text{cation-radical} \quad (6)$$

Accumulation and stabilization of the cation-radicals near the electrode leads not only to stop the dark hole injection, but also to a drop of dark conductivity, increase the V value, as well as to the observation of photo-stimulated currents (PSC), which manifest themselves as growth of PES in the red spectral range S_{red}, outside the absorption band of the CTC (absorption of cation-radicals) (Figure 3):

$$\text{Cation-radical} + h\upsilon_1 \xrightarrow{\text{FATD}} IP_1 \rightarrow \text{curriers (PSC)} \quad (7)$$

The growth of S_{red} with increasing N (Figure 3) is partly due to its field dependence caused by growth of the field strength E = V/d. Therefore, it was specially checked that in the red region the pure field dependence due to the ion pair IP_1 FATD (7) have the form: $\beta \sim E^n$ (n = 1.35-1.60) and by (2) $S \sim E^{n-1}$, i.e. weakly dependent on E, so that the growth of $S_{red}(N)$ is partly due to the accumulation of the cation-radicals. Under conditions when V does not depend on N (for N > 10), the V value was changing by varying the time of corona discharge. In some cases (Figure 5) the growth of S_{red} was observed at constant V that points directly to the effect of the cation-radical accumulation.

The observation of PSC indicates a high cation-radical lifetime, $t > (\sigma I)^{-1}$ (σ - absorption cross section). If $\sigma = 10^{-17} – 10^{-16}$ cm^2 [5], I = 10^{15} cm^{-2} s^{-1}, an estimate of t > 10 s is obtained. It should be noted that the results of this study evidences that there is a range of the cation-radical states from labile (t = 1-10 s) to a fully stable ones (t > 10^3 s) which are involved in the process of photo-stimulated generation. Similar stabilized cation-radicals and related photo-stimulated currents for the PI based on substituted triphenylamines resulting from irreversible photochemical transformation of free-radical type with the halogen hydrocarbons are observed in [45].

Conclusions

A novel conjugated polymers, polyimides based on N,N',N'',N'''-substituted paraphenylenediamine and dianhydrides of aromatic tetracarboxylic acids, was successfully prepared via Suzuki coupling reaction. The polymer exhibits excellent solubility in common organic solvent, and has high thermal stability such as T_{d10} at 453 ^{0}C in nitrogen atmosphere and T_g at about 140 ^{0}C.

The photoelectric sensitivity of the PI films (3 μm thickness) is observed in the UV, and visible spectral regions, due to the interactions with charge transfer between donor and acceptor fragments of the PI chains (formation of CTC). Study of the photogeneration quantum yield field dependence gives the evidence that the photo-generation mechanism is a field assisted thermo-dissociation of radical ion pairs kinetically associated with the excited CTC.

The second important mechanism of photogeneration is photostimulation of long-lived stable cation-radicals of the donor PI fragments, representing the hole (major carriers) captured by deep centers (photo-stimulated currents). Accumulation of the cation-radicals in the dark and photo-processes leads to the dependence of photovoltaic characteristics on the number of charge-discharge cycles of the sample.

Appendix 1

Materials:

N,*N*,-bis(4-aminohenyl)-*N'*,*N'*-bis[4-(2-phenyl-2-isopropyl)phenyl]-1,4-phenylene diamine was synthesized by a well-known synthetic route starting from bis(4-tert-butylphenyl)amine and p-fluoronitrobenzene as shown in Scheme 1 [43]. The synthetic details and the characterization data of this diaminemonomer have been described in [43]. Bis[4-(2-phenyl-2-isopropyl)phenyl]amine (OUCHI SHINKO), 4-fluoro-nitro- benzene (ACROS), cesium fluoride (ACROS), sodium hydride (95%; dry; ALDRICH), 10% Pd/C (MERCK), and hydrazine monohydrate (MERCK) were used as received. *N*,*N*-Dimethylacetamide (DMAc; MERCK), dimethyl sulfoxide (DMSO), *N*-methyl-2-pyrrolidinone (NMP) (MERCK), and pyridine (MERCK), were dried over calcium hydride overnight, distilled under reduced pressure, and stored over 4 Å molecular sieves in a sealed bottle. Iodobenzene, bis(dibenzylideneacetone) palladium [Pd(dba)$_2$], 1,1'-

bis(diphenylphosphino)-ferrocene (DPPF), sodium *tert*-butoxide were purchased from ACROS. Commercially available aromatic tetracarboxylic dianhydrides such as 4,4′-hexafluoroisopropylidenediphathalic dianhydride (**A1**; CHRISKEV) (6FDA), 3,3′,4,4′-diphenyl sulfone-tetracarboxylic dianhydride (**A2**; TCI) (DSDA), 4,4′-oxydiphthalic anhydride (**A3**; TCI) (ODPA), 3,3′,4,4′-benzophenone tetracarboxylic dianhydride (**A4**; CHRISKEV) (BTDA) and 3,3′,4,4′-bitetracarboxylic dianhydride (**A5**; CHRISKEV) (BDA), and were purified by vacuum sublimation.

Appendix 2

Monomer synthesis[35]

Synthesis of bis[4-(2-phenyl-2-isopropyl)phenyl]-4-nitrophenylamine) (1). In a 500 mL three neck round-bottom flask was placed bis[4-(2-phenyl-2-isopropyl)phenyl]amine (20.0 g, 49 mmol), 4-fluoro-nitrobenzene (5.23 g, 49 mmol), sodium hydroxide (1.18 g, 49 mmol), and 120 mL DMSO. The mixture was heated with stirring at 120 °C for 24 h. The reaction mixture was cooled and then poured into 1 liter methanol. The yellow precipitate was collected by filtration and dried under vacuum. The product was purified by silica gel column chromatography (*n*-hexane : dichloromethane = 2 : 1) to afford nitro compound **1** 16.3 g in a 63 % yield; mp 150-151 °C by DSC (10 °C /min).

IR (KBr): 1585, 1342 cm^{-1} (NO_2 stretch).

^{1}H NMR: (DMSO-d_6): δ (ppm)=1.77 (s, 6H, H_d); 6.93-6.95 (d, 1H, H_f, *J*=9.5 Hz); 7.12-7.14 (d, 2H, H_e, *J*=10.1 Hz); 7.24-7.27 (m, 1H, H_a); 7.28-7.30 (d, 2H, H_d, *J*=10.1 Hz); 7.35-7.36 (d, 2H, H_b, *J*=5.0 Hz); 7.37-7.38 (d, 2H, H_c, *J*=5.0 Hz); 8.05-8.08 (d, 1H, H_g, *J*=15.0 Hz).

^{13}C NMR (DMSO-d_6): δ (ppm)=30.6 (C_6), 42.6 (C_5), 117.4 (C_{12}), 125.3 (C_{13}), 125.7 (C_1), 125.9 (C_9), 126.6 (C_2), 128.0 (C_3), 128.1 (C_8), 139.6 (C_{14}), 142.8 (C_{10}), 148.2 (C_7), 150.0 (C_4), 153.4 (C_{11}).

Anal. Calcd for $C_{36}H_{34}N_2O_2$: C, 82.10%; H, 6.51%; N, 5.32%. **Found**: C, 81.67%; H, 6.39%; N, 5.21%.

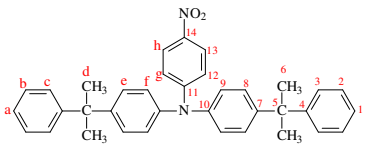

(**1**)

Synthesis of bis[4-(2-phenyl-2-isopropyl)phenyl]-4-aminophenylamine (2). In a 500 mL three neck round-bottom flask was placed nitro compound **1** (20 g, 38 mmol), Pd/C (0.4 g), ethanol 200 mL. After the addition of 14 mL of hydrazine monohydrate, the solution was stirred at reflux temperature for 12 h. After the solution was cooled down to room temperature, the solution was filtered to remove the catalyst, and the crude product was recrystallized from ethanol yielded 12.5 g (yield: 66%) of the compound **2,** mp 110-114℃ by DSC (10 °C /min).

IR (KBr): 3432, 3356 cm^{-1} (NH_2 stretch).

^{1}H NMR: (DMSO-d_6): δ (ppm)= 1.57 (s, 6H, H_h); 5.02 (s, 1H, NH_2); 6.56-6.58 (d, 1H, H_g, *J*=8.5 Hz); 6.76-6.77 (d, 1H, H_f, *J*=5.0 Hz); 6.77-6.79 (d, 2H, H_e, *J*=10.0 Hz); 6.98-7.00 (d, 2H, H_d, *J*=10.0 Hz); 7.09-7.12 (m, H, H_a); 7.19-7.20 (d, 2H, H_b, *J*=5.0 Hz); 7.20-7.21 (d, 2H, H_c, *J*=5.0 Hz).

^{13}C NMR (DMSO-d_6): δ (ppm)= 30.3 (C_6), 41.7 (C_5), 114.9 (C_{13}), 120.73 (C_9), 125.3 (C_1), 126.2 (C_3), 126.9 (C_8), 127.8 (C_2), 127.9 (C_{12}), 135.2 (C_{14}), 142.5 (C_{10}), 145.4 (C_7), 145.9 (C_{11}), 150.3 (C_4).

E_{LEM}. A_{NAL}. Calcd. For $C_{36}H_{36}N_2$: C, 87.05%; H, 7.31%; N, 5.64%. **Found:** C, 86.9%; H, 7.13%; N, 5.61%.

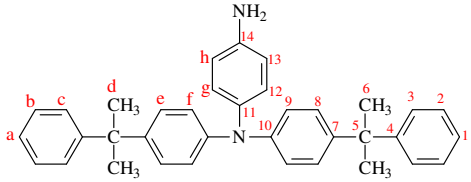

(**2**)

Synthesis of N,N,-bis(4-nitrophenyl)-N′,N′-bis[4-(2-phenyl-2-isopropyl)phenyl]-1,4-phenylene-diamine (3). In a 250 mL three neck round-bottom flask was placed bis- [4-(2-phenyl- 2-isopropyl)phenyl]-4-aminophenylamine **(2)** (7.26 g, 14.63 mmol), 4-fluoro-nitro- benzene (4.13 g, 29.27 mmol), cesium fluoride (4.41 g, 29.27 mmol), and 80 mL DMSO. The mixture was heated with stirring at 120 °C for 24 h. The reaction mixture was cooled and then poured into 500 mL methanol. The red precipitate was collected by filtration and dried under vacuum. The product was purified by silica gel column chromatography (*n*-hexane : dichloromethane = 1: 1) to afford dinitro compound (**3**) in a 65% yield; mp 224-225 °C (by DSC; 10 °C /min).

IR (KBr): 1580, 1341 cm^{-1}(NO_2 stretch).

^{1}H NMR ($CDCl_3$): δ (ppm)= 1.70 (s, 6H, H_d); 6.97-6.99 (d, 2H, H_h, *J*=10.0 Hz); 7.04-7.05 (d, 2H, H_f, *J*=5.0 Hz); 7.05-7.07 (d, 2H, H_g, *J*=10.0 Hz); 7.15-7.17 (d, 2H, H_e, *J*=10.0 Hz); 7.19-7.20 (d, 2H, H_i, *J*=5.0 Hz); 7.20-7.21 (m, 1H, H_a); 7.28-7.29 (d, 2H, H_c, *J*=5.0 Hz); 7.30-7.31 (d, 2H, H_b, *J*=5.0 Hz); 8.14-8.17 (d, 2H, H_j, *J*=15.0 Hz).

^{13}C NMR ($CDCl_3$): δ (ppm)= 30.7 (C_6), 42.5 (C_5), 121.8 (C_{16}), 123.2 (C_{12}), 124.3 (C_9), 125.4 (C_{17}), 125.6 (C_1), 126.6 (C_3), 127.7 (C_8), 127.9 (C_2), 128.0 (C_{13}), 137.2 (C_{14}), 142.3 (C_{18}), 144.3 (C_{10}), 146.1 (C_7), 147.0 (C_{11}), 150.4 (C_4), 151.7 (C_{15}).

E_{LEM}. A_{NAL}. Calcd. For $C_{48}H_{42}N_4O_4$: C, 78.03 %; H, 5.73%; N, 7.58%. **Found**: C, 77.57%; H, 5.63%; N, 7.45%.

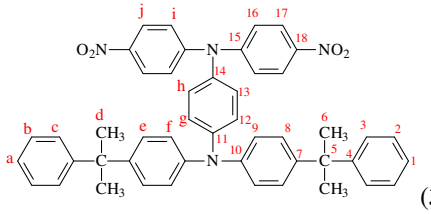

(**3**)

Synthesis of N,N,-bis(4-aminohenyl)-N′,N′-bis[4-(2-phenyl-2-isopropyl)phenyl]-1,4-phenylene-diamine (4). The dinitro compound **(3)** (5 g, 6.77 mmol), Pd/C (0.2 g), and 150 mL ethanol were taken in a three-necked flask and hydrazine monohydrate (10 mL) was added dropwise over a period of 30 min at 90 °C. Upon completing the addition, the solution was stirred at reflux temperature for 12 h. After the solution was cooled down to room temperature, the solution was filtered to remove the catalyst, and the crude product was purified by silica gel column chromatography (*n*-hexane : ethyl acetate = 2: 1) to afford diamine monomer (**4**) 2.3 g (yield: 50%), mp 149-151 °C by DSC (10 °C /min).

IR (KBr): 3445, 3360 cm^{-1}(NH_2 stretch).

^{1}H NMR (DMSO-d_6): δ (ppm)= 1.56 (s, 6H, H_d); 6.53-6.55 (d, 2H, H_f, *J*=10.1 Hz); 6.56-6.58 (d, 1H, H_h, *J*=10.1 Hz); 6.75-6.77 (d, 1H, H_g, *J*=10.1 Hz); 6.77-6.79 (d, 2H, H_i, *J*=10.1 Hz,); 6.80-6.82 (d, 2H, H_e, *J*=10.1 Hz); 6.99-7.01 (d, 2H, H_j, *J*=10.1 Hz); 7.09-7.12 (m, 1H, H_a); 7.19-7.20 (d, 2H, H_c, *J*=5.1 Hz); 7.21-7.23 (d, 2H, H_b *J*=10.1 Hz).

^{13}C NMR (DMSO-d_6): δ (ppm)= 30.3 (C_6), 41.7 (C_5), 114.8 (C_8), 117.8 (C_{13}), 121.3 (C_{16}), 125.3 (C_1), 126.2 (C_3), 126.7 (C_{12}), 127.0 (C_9), 127.1 (C_{17}), 127.8 (C_2), 136.0 (C_{10}), 137.2 (C_{14}), 143.0 (C_{18}), 145.2 (C_{15}), 145.3 (C_7), 146.2 (C_{11}), 150.2 (C_4).

E_{LEM}. A_{NAL}. Calcd. For $C_{48}H_{46}N_4$: C, 84.92%; H, 6.83%; N, 8.25%. **Found**: C, 84.11%; H, 6.77%; N, 8.17%.

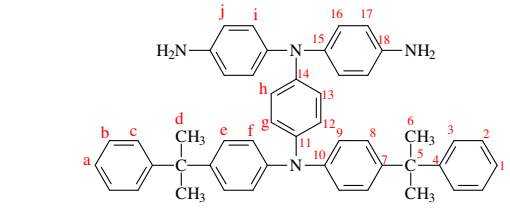

(4)

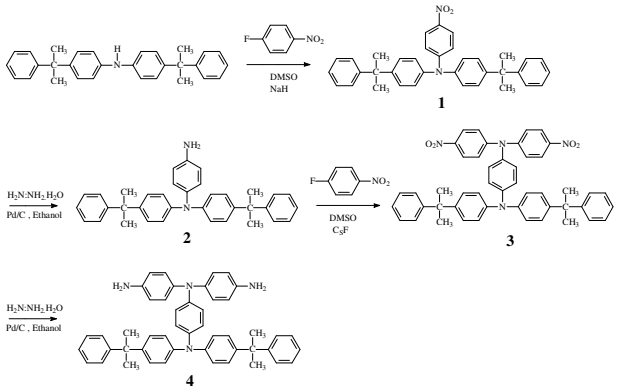

Appendix 3

The IR spectrum of **A1** (film) exhibited characteristic imide absorption at 1779 (asymmetrical carbonyl stretching), 1726 (symmetrical carbonyl stretching) and 744 cm^{-1} (imide ring deformation).

^{1}H NMR ($CDCl_3$): δ (ppm)= 1.70 (s, 6H, H_d); 7.02-7.04 (d, 2H, H_f); 7.04-7.10 (d, 2H, H_h + H_g); 7.13-7.14 (d, 2H, H_e); 7.16-7.20 (m, 1H, H_a); 7.27-7.28 (d, 2H, H_i); 7.27-7.30 (d, 4H, H_b + H_c); 7.32-7.33 (d, 2H, H_j); 7.88-7.90 (d, 2H, H_l); 7.99 (s, 1H, H_k); 8.05-8.07 (d, 2H, H_m).

E_{LEM}. A_{NAL}. Calcd. For $(C_{69}H_{54}N_5O_4F_6)_n$: C, 74.18%; H, 4.87%; N, 5.01%. **Found**: C, 73.01%; H, 4.23%; N, 5.02%.

Acknowledgements. This work supported by RFBR grants 10-02-92000-NNC_a, 11-02-00868-a, 11-02-12041-OFI-m-2011 and grant of the Ministry of Education and Science of the RF 1B-5-343.

References

1. Beaujuge P.M., Vasilyeva S.V., Ellinger S., McCarley T.D., Reynolds J.R. // Macromolecules 2009, V. 42, P. 3694–3706.
2. Han, F. S.; Higuchi, M.; Kurth, D. G. // Adv Mater 2007, 19, 3928–3931.
3. Udum, Y. A.; Yildiz, E.; Gunbas, G.; Toppare, L. // J Polym Sci Part A: Polym Chem 2008, 46, 3723–3731.
4. Thompson, B. C.; Kim, Y. G.; McCarley, T. D.; Reynolds, J. R. // J Am Chem Soc 2006, 128, 12714–12725.
5. Michinobu, T.; Kumazawa, H.; Otsuki, E.; Usui, H.; Shigehara, K. // J Polym Sci Part A: Polym Chem 2009, 47, 3880–3891.
6. Elschner, A.; Heuer, H. W.; Jonas, F.; Kirchmeyer, S.; Wehrmann, R.; Wussow, K. // Adv Mater 2001, 13, 1811–1814.
7. Winter, A.; Friebe, C.; Chiper, M.; Hager, M. D.; Schubert, U.S. // J Polym Sci Part A: Polym Chem 2009, 47, 4083–4098.
8. Forrest, S. R. // Nature 2004, 428, 911–918.
9. Liao, L.; Cirpan, A.; Chu, Q.; Karase, F. E.; Pang, Y. // J Polym Sci Part A: Polym Chem 2007, 45, 2048–2058.
10. Yu, G.; Gao, J.; Hummelen, J. C.; Wudl, F.; Heeger, A. J. // Science 1995, 270, 1789–1791.
11. Kitamura, M.; Arakawa, Y. // Appl Phys Lett 2009, 95, 023503–02503(3).
12. Dimitrakopoulos, C. D.; Malenfant, P. R. L. // Adv Mater 2002, 14, 99–117.
13. Liu, P.; Wu, Y.; Pan, H.; Li, Y.; Gardner, S.; Ong, B. S.; Zhu, S. // Chem Mater 2009, 21, 2727–2732.
14. Roberts, M. E.; LeMieux, M. C.; Sokolov, A. N.; Bao, Z. // Nano Lett 2009, 9, 2526–2531.
15. Durben, S.; Nickel, D.; KruË ger, R. A.; Sutherland, T. C.; Baumgartner, T. // J Polym Sci Part A: Polym Chem 2008, 46, 8179–8190.
16. Segura, J. L.; Martin, N.; Guldi, D. M. // Chem Soc Rev 2005, 34, 31–47.
17. Chang, Y. T.; Hsu, S. L.; Su, M. H.; Wei, K. H. // Adv Mater 2009, 21, 2093–2097.
18. Zhou, E. J.; Tan, Z. A.; He, Y. J.; Yang, C. H.; Li, Y. F. // J Polym Sci Part A: Polym Chem 2007, 45, 629–638.
19. Ling, Q. D.; Liaw, D. J.; Zhuc, C.; Chanc, D. S. H.; Kang, E. T.; Neoh, K. G. Prog Polym Sci 2008, 33, 917–978.
20. Ling, Q. D.; Liaw, D. J.; Teo, E. Y. H.; Zhu, C.; Chan, D. S. H.; Kang, E. T.; Neoh, K. G. // Polymer 2007, 48, 5182–5201.
21. Scherf, U.; List, E. J. W. // Adv Mater 2002, 14, 477–487.
22. Naga, N.; Tagaya, N.; Noda, H.; Imai, T.; Tomoda, H. // J Polym Sci Part A: Polym Chem 2008, 46, 4513–4521.
23. Wang, B.; Shen, F.; Lu, P.; Tang, S.; Zhang, W.; Pan, S.; Liu, M.; Liu, L.; Qiu, S.; Ma, Y. // J Polym Sci Part A: Polym Chem 2008, 46, 3120–3127.

24. Xu, Y.; Guan, R.; Jiang, J.; Yang, W.; Zhen, H.; Peng, J.; Cao, Y. // J Polym Sci Part A: Polym Chem 2008, 46, 453–463.
25. Ranger, M.; Rondeau, D.; Leclerc, M. // Macromolecules 1997, 30, 7686–7691.
26. Janietz, S.; Bradley, D. D. C.; Grell, M.; Giebeler, C.; Inbasekaran, M.; Woo, E. P. // Appl Phys Lett 1998, 73, 2453–2455.
27. Posadas, D.; Florit, M. I. // J Phys Chem B 2004, 108, 15470–15476.
28. Sonmez, G.; Wudl, F. // J. Mater Chem 2005, 15, 20–22.
29. Rosseinsky, D. R.; Montimer, R. // J. Adv Mater 2001, 13, 783–793.
30. Durmus, A.; Gunbas, G. E.; Camurlu, P.; Toppare, L. // Chem Commun 2007, 31, 3246–3248.
31. Ogino, K.; Kanagae, A.; Yamaguchi, R.; Sato, H.; Kurtaja, // J. Macromol Rapid Commun 1999, 20, 103–106.
32. Yu, W. L.; Pei, J.; Huang, W.; Heeger, A. // J. Chem Commun 2000, 8, 681–682.
33. Chou, M. Y.; Leung, M. K.; Su, Y. O.; Chiang, S. L.; Lin, C. C.; Liu, J. H.; Kuo, C. K.; Mou, C. Y. // Chem Mater 2001, 16, 654–661.
34. Wu, H.-U., Wang K.-L., Liaw, D.-J., Lee, K.-R., Lai, J.-Y. // J. Polym Sci: Part A: Polym Chem, 2010, 48, 1469–1476.
35. Kotov B.V., Berendyaev V.I., Rumyantsev B.M., Bespalov B.P., Lunina E.V., Vasilenko N.A. Molecular Design of Highly Sensitive Soluble Photoconductive Polyimides. // Doklady RAS, Physical Chemistry, 1999, v.367, p.183-187.
36. Rumyantsev B.M., Berendyaev V.I., Tsegel'skaya A.Yu., Kotov B.V. Molecular Aggregate Formation and Microphase Segregation Effects on the Photoelectrical and Photovoltaic Properties of Polyimide-Perylenediimide Composite Films. // Mol. Cryst. Liq. Cryst., 2002, v.384, p.61-67.
37.Rumyantsev B.M., Berendyaev V.I., Golub A.S., Lenenko N.D., Novikov Yu.N., Krinichnaya E.P., Zhuravleva T.S. Organic-Inorganic Polymer Nanocomposites for Photovoltaics. J. High Energy Chem. 2008, v.42, № 7, p.61-63.
38. Mal'tsev E.I., Berendyaev V.I., Brusentseva M.A., Tameev A.R., Kolesnikov V.A., Kozlov A.A., Kotov B.V., Vannikov A.V. Aromatic Polyimides as Efficient Materials for Organic Electroluminescent Devices. // Polym. International. 1997, v.42, p.404.
39. Muhlbacher D., Brabec C.J., Sariciftsi N.S., Kotov B.V., Berendyaev V.I., Rumyantsev B.M., Hummelen J.C. Sensitization of Photoconductive Polyimides for Photovoltaic Applications. // Synth. Metals. 2001, v.121, p.1550-1551.
40. Rumyantsev B.M., Berendyaev V.I. Organic Polymer *p-n* Heterostructures for Optoelectronics // J. Chem. Phys. (Russian) in press.
41. Marjanovich N., Singh Th.B., Deunler G., Gunes S., Neugebauer H., Sariciftsi N.S. Schwodianer R., Bauer S. Photoresponse of Organic Field-Effect Transistors Based on Conjugated Polymer /Fullerene Blends. // Organic Electronics. 2006, v.7, issue 4, p.188-194.
42. Grenishin S.G. Electrophotographic process. M.: Science. 1970, 374 p.
43. Chang, C.-H., Wang, K.-L., Jiang, J.-C., Liaw, D.-J., Lee, K.-R., Lai, J.-Y., Lai, K.-H. // Polymer 2010, 51, 4493-4502.
44. Rumyantsev B.M., Berendyaev V.I., Vasilenko N.A., Malenko S.V., Kotov B.V. Photogeneration of Charge Carriers in Layers of Soluble Photoconducting Polyimides and Their Sensitization by Dyes. // Polymer Science, Ser. A, 1997, v.39, №4, p.506-512.
45. Rumyantsev B.M., Berendyaev V.I., Kotov B.V. Photoconduction Kinetics and Nature of Intermediate Photogeneration Centers in Soluble Photoconductive Polyimides. // J. Phys. Chem. Photochemistry and Magnetochemistry (Russian). 1999, v.73, №3, p. 538-547.
Icentific
46. Relaxation in Polymers. Edited by T. Kobayashi. World Scientific. Singapore, 1993, 329 p.
47. Semiconductors and Semimetals. V. 85. Quantum Efficiency in Complex Systems. Part II. From Molecular Aggregates to Organic Solar Cells. Edited by U. Wurfel, M. Thowart and E. Weber. Elsevier, 2011, 341 p. Chapter 9, p. 312.

© **A. A. Olkhov –** PhD, docent, Moscow Plekhanov Russian University of Economics, Moscow, Russia, aolkhov72@yandex.ru; **B. M. Rumyantsev -** Dr.sc.(Tech.), Prof Institute of Chemical Physics, RAS, Moscow, Russia; **G. E. Zaikov -** Dr.sc.(chemistry), Prof., Institute of Biochemical Physics, RAS, Moscow, Russia, gezaikov@yahoo.com; **A. A. Ischenko -** Dr.sc.(chemistry), Prof., Moscow Lomonosov State University of Fine Chemical Technology, Moscow, Russia; **V. F. Shkodich –** Ph.D, Assoc. Professor Department of technology of synthetic rubber, Kazan National Research Technological University, shkodich@mail.ru; **A. M. Kochnev -** Professor Department of technology of synthetic rubber, Kazan National Research Technological University, kochnev55@bk.ru.